

Longitudinal Assessment of Structural Phenotype in Brugada Syndrome Using Cardiac Magnetic Resonance Imaging

Julia C. Isbister, MBBS,^{*†‡} Belinda Gray, BSc (Med), MBBS,^{†‡}
 Sophie Offen, BSc, MBBS,^{†‡} Laura Yeates, BSc (hons), GradDipGenCouns,^{*†‡§¶}
 Chris Naoum, MBBS, PhD,^{||} Caroline Medi, BMed, PhD,^{†‡}
 Hariharan Raju, MBChB, PhD,^{†||**} Christopher Semsarian, MBBS, PhD, MPH, FHRS,^{*†‡}
 Rajesh Puranik, MBBS, PhD,^{†‡} Raymond W. Sy, MBBS, PhD, FHRS^{†||}

From the ^{*}Agnes Ginges Centre for Molecular Cardiology at Centenary Institute, University of Sydney, Sydney, New South Wales, Australia, [†]Faculty of Medicine and Health, University of Sydney, Sydney, New South Wales, Australia, [‡]Department of Cardiology, Royal Prince Alfred Hospital, Sydney, New South Wales, Australia, [§]Centre for Population Genomics, Garvan Institute of Medical Research, University of New South Wales, Sydney, New South Wales, Australia, [¶]Centre for Population Genomics, Murdoch Children's Research Institute, Melbourne, Victoria, Australia, ^{||}Department of Cardiology, Concord Repatriation General Hospital, Sydney, New South Wales, Australia, and ^{**}Faculty of Medicine, Health and Human Sciences, Macquarie University, Sydney, New South Wales, Australia.

BACKGROUND Despite historically being considered a channelopathy, subtle structural changes have been reported in Brugada syndrome (BrS) on histopathology and cardiac magnetic resonance (CMR) imaging. It is not known if these structural changes progress over time.

OBJECTIVE The study sought to assess if structural changes in BrS evolve over time with serial CMR assessment and to investigate the utility of parametric mapping techniques to identify diffuse fibrosis in BrS.

METHODS Patients with a diagnosis of BrS based on international guidelines and normal CMR at least 3 years prior to the study period were invited to undergo repeat CMR. CMR images were analyzed de novo and compared at baseline and follow-up.

RESULTS Eighteen patients with BrS (72% men; mean age at follow-up 47.4 ± 8.9 years) underwent serial CMR with an average of 5.0 ± 1.7 years between scans. No patients had late gadolinium enhancement (LGE) on baseline CMR, but 4 (22%) developed LGE on

follow-up, typically localized to the right ventricular (RV) side of the basal septum. RV end-systolic volume increased over time ($P = .04$) and was associated with a trend toward reduction in RV ejection fraction ($P = .07$). Four patients showed a reduction in RV ejection fraction >10%. There was no evidence of diffuse myocardial fibrosis observed on parametric mapping.

CONCLUSIONS Structural changes may evolve over time with development of focal fibrosis, evidenced by LGE on CMR in a significant proportion of patients with BrS. These findings have implications for our understanding of the pathological substrate in BrS and the longitudinal evaluation of patients with BrS.

KEYWORDS Brugada syndrome; Cardiac magnetic resonance; Cardiomyopathy; Fibrosis; Late gadolinium enhancement

(Heart Rhythm 0² 2022; ■:1–8) © 2022 Heart Rhythm Society. Published by Elsevier Inc. This is an open access article under the CC BY-NC-ND license (<http://creativecommons.org/licenses/by-nc-nd/4.0/>).

Brugada syndrome (BrS) is an inherited heart disease characterized by an electrocardiogram (ECG) signature of down-sloping ST-segment elevation with T-wave inversion in the right precordial leads and a risk of malignant ventricular arrhythmia.^{1,2} BrS has primarily been considered a channelopathy due to its signature ECG phenotype, the absence of ubiq-

uitous structural disease, and its association with pathogenic variants in the *SCN5A* gene. However, structural abnormalities in BrS are increasingly appreciated. Histopathological changes including fibrosis, fatty infiltration, inflammatory infiltrates, and increased collagen deposition have been described in patients with BrS.^{3–6} Structural changes have also been observed with cardiac magnetic resonance (CMR) imaging, which is the gold standard for right ventricular (RV) assessment and noninvasive detection of replacement fibrosis.^{7–10} Newer parametric mapping techniques allow

Address reprint requests and correspondence: Dr Raymond Sy, University of Sydney, Camperdown, NSW, 2006, Australia. E-mail address: raymond.sy01@gmail.com.

KEY FINDINGS

- Focal fibrosis evidenced by late gadolinium enhancement on cardiac magnetic resonance and a subtle increase in right ventricular volumes can develop during follow-up in Brugada syndrome.
- Findings suggest a progressive myocardial pathology in some patients with Brugada syndrome.
- Current parametric mapping techniques do not appear to detect diffuse fibrosis in patients with Brugada syndrome.

more detailed tissue characterization for subtle changes such as diffuse fibrosis, but these have not been specifically studied in BrS.¹¹

In inherited cardiomyopathies such as hypertrophic cardiomyopathy (HCM), disease penetrance has been shown to be age related.¹² Indeed, the extent of structural abnormalities in HCM, including focal myocardial scar, can progress over time, and these changes correlate with clinical outcomes.¹³ In BrS, the first arrhythmic events most often occur in the third or fourth decade of life, and structural abnormalities identified on noninvasive imaging may correlate with arrhythmic events.^{2,14} Hence, it is important to assess whether the structural abnormalities in BrS emerge or progress over time.

In this exploratory study, we sought to identify if the structural changes in patients with BrS develop or progress over time on serial CMR imaging. The secondary aim was to investigate if newer parametric mapping CMR techniques may detect diffuse fibrosis in BrS.

Methods

Patient selection

Patients who fulfilled diagnostic criteria for BrS, 2-mm coved-type ST-segment elevation spontaneously or after provocation with sodium-channel blocker, were recruited from the Genetic Heart Disease Clinic at Royal Prince Alfred Hospital, Sydney, Australia.¹ Patients with BrS were invited to participate if they had undergone CMR imaging more than 3 years prior demonstrating normal ventricular volumes and absence of myocardial scar, and if there were no contraindications to repeat scanning such as an implantable cardioverter-defibrillator. Notably, no patients screened for inclusion were excluded due to abnormal baseline volumes or baseline late gadolinium enhancement (LGE), in keeping with the subclinical volumetric changes described in BrS and low rate of LGE previously described.⁹ Demographic and clinical information were collected from patient records. Patients with no history of cardiac arrest or syncope were considered asymptomatic and a family history of sudden cardiac death was noted if a first- or second-degree relative died suddenly under the age of 45 years. The study adhered to Helsinki Declaration guidelines, was approved by the local

research ethics committee (X15-0061), and informed consent was obtained from all participants.

CMR acquisition

Baseline CMR scans were obtained for *de novo* analysis. Follow-up CMR scans were performed using a 1.5T (Philips, Best, the Netherlands) scanner, and the imaging protocol included steady-state free precession cine acquisitions of both ventricles from base to apex in the vertical long-axis, 4-chamber, and short-axis views. Segmented phase-sensitive inversion recovery sequences (imaging parameters: repetition time = 3.6 ms; echo time = 1.2 ms; flip angle = 15°; slice thickness = 5 mm; field of view = 370 mm, acquired during a single breath hold) were used to identify focal myocardial scar 10 minutes postadministration of intravenous contrast (0.2 mmol/kg of gadobutrol [Gadovist]). A Look-Locker sequence was used to determine the null point of normal remote myocardium. Significant enhancement was defined as occurring at 5 SDs above the null point. Parametric mapping was performed for tissue characterization on follow-up scans (required sequences were not available at the time of baseline scanning). Native T1 times were computed in the interventricular septum, and hematocrit was measured immediately prior to scanning using a point-of-care device for extracellular volume (ECV).

CMR analysis

Image analysis was performed using Horos version 3.3 (Horos Project; <https://horosproject.org/>) and OsiriX 12 (Pixmeo SARL, Geneva, Switzerland). The presence or absence of LGE was reported independently by 2 level 3 European Association of Cardiovascular Imaging/Society for Cardiovascular Magnetic Resonance reporters. Native T1 times and ECV were compared with the local reference range (native T1 = 968–1076 ms and ECV <28%). Left ventricular (LV) and RV volumes and ejection fractions (EFs) were calculated using Simpson's method after manually contouring the endocardial surface at end-diastole and end-systole in sequential cine short-axis slices. Ventricular volumes were compared with reference standards for age and sex, according to standard recommendations.^{15,16} A change in EF ≥10 percentage points was considered a significant change over time. This cutoff was chosen on the basis of the reported reproducibility of EF measurements, and consensus definitions of LV impairment in the cardio-oncology setting.^{17,18} RV outflow tract (RVOT) volume was assessed on short-axis images by manual segmentation in end-diastole. For consistency, the inferior border of the RVOT was taken at 90° from the LV or RV insertion points or RV or aortic junction as appropriate. The superior border was defined at the level of the pulmonary valve. RVOT volume was derived using Simpson's method. RVOT volume was measured twice on all scans, and the mean volume is reported. RVOT volume was then calculated on a random selection of 20% of CMR images by a second observer for the appraisal of interobserver variability.

Table 1 Cohort characteristics (N = 18)

Male	13 (72)
Age at baseline, y	42.4 ± 8.8
Age at follow-up, y	47.4 ± 8.9
Asymptomatic	18 (100)
Spontaneous type 1 ECG	9 (50)
Shanghai score	3.0 ± 0.9
Family history of BrS	3 (17)
Family history of SCD	1 (6)
SCN5A positive*	3 (19)
Quinidine therapy	4 (22)
Time between CMR imaging, y	5.0 ± 1.7

Values are n (%) or mean ± SD.

BrS = Brugada syndrome; CMR = cardiac magnetic resonance; ECG = electrocardiogram; SCD = sudden cardiac death.

*SCN5A status of 2 patients was unknown.

Statistical analysis

SAS OnDemand (SAS Institute, Cary, NC) and GraphPad Prism version 9.1 (GraphPad Software, San Diego, CA) were used for statistical analysis. Descriptive statistics of continuous variables are reported as mean ± SD and categorical variables are reported count and percentage of available data. Continuous variables were tested for normality using the Shapiro-Wilk test and compared using 2-tailed, paired *t* tests. Statistical significance was defined as *P* < .05. The data underlying this article will be shared on reasonable request to the corresponding author.

Results

Patient characteristics

The clinical characteristics of the cohort are reported in [Table 1](#). The majority of participants were men (72%), and the average age at time of follow-up scan was 47.4 ± 8.9 years. Given the exclusion of patients with implantable

cardioverter-defibrillators, all patients were asymptomatic. Nine (50%) patients had a spontaneous type 1 BrS ECG pattern, 2 (11%) patients had a history of fever-induced type 1 pattern, and 7 (39%) had only a type 1 BrS ECG documented during a sodium-channel blocker challenge. Three patients had a pathogenic or likely pathogenic *SCN5A* variant (patient WC1: c.1936delC; patient AOL1: c.4086delG; patient TD3 had a previously described balanced translocation interrupting *SCN5A*).^{19,20}

CMR analysis: Volumetric assessment

CMR indices at baseline and follow-up are detailed [Table 2](#). Although all volumetric indices were within the normal range at baseline and follow-up, there was an increase in RV end-systolic volume (RVESV) from baseline to follow-up scan (63.1 ± 26.6 mL to 71.2 ± 21.7 mL; *P* = .04) that persisted after indexing for body surface area (*P* = .050), as illustrated in [Figure 1A](#). A trend toward reduction in RVEF over time was also observed (58.1 ± 7.0% to 54.6 ± 5.2%; *P* = .07) ([Figure 1B](#)). Four patients had an absolute reduction in RVEF by more than 10%, and clinical characteristics of these patients are reported in [Table 3](#). Mean RVOT volumes increased on follow-up scans, but the change was not statistically significant. Intra- and interobserver correlation coefficients for RVOT end-diastolic volume were 0.91 and 0.74, respectively. Baseline and follow-up CMR parameters were similar between patients with spontaneous type 1 ECG pattern and those with an inducible type 1 ECG pattern ([Supplemental Tables 1 and 2](#)). There were no significant differences in LV volumes or LVEF.

CMR analysis: Fibrosis assessment

No patients had evidence of LGE on the baseline scan. Four (22%) patients developed LGE on follow-up CMR

Table 2 CMR indices at baseline and follow-up

	Normal range	Baseline	Follow-up	<i>P</i> value
Body surface area	—	1.9 ± 0.2	1.9 ± 0.3	.313
LVEDV, mL	77–195	129.7 ± 37.7	130.9 ± 32.6	.765
LVEDVi, mL/m ²	47–92	66.9 ± 15.4	66.8 ± 9.6	.962
LVESV, mL	19–72	44.6 ± 16.9	46.9 ± 15.8	.356
LVESVi, mL/m ²	13–30	22.9 ± 7.2	24.4 ± 5.1	.305
LVEF, %	56–78	66.1 ± 6.4	64.6 ± 6.7	.375
RVEDV, mL	88–227	147.4 ± 46.0	155.1 ± 40.3	.126
RVEDVi, mL/m ²	47–92	75.9 ± 18.4	78.8 ± 11.4	.294
RVESV, mL	23–103	63.1 ± 26.6	71.2 ± 21.7	.041*
RVESVi, mL/m ²	15–45	32.1 ± 11.6	36.2 ± 7.4	.050*
RVEF, %	47–74	58.1 ± 7.0	54.6 ± 5.2	.071
RVOT-EDV, mL	NA	10.3 ± 4.8	11.3 ± 3.7	.189
RVOT-EDVi, mL/m ²	NA	5.0 ± 2.5	5.8 ± 1.6	.215
RVOT as proportion of RVEDV, %	NA	6.8 ± 2.1	7.4 ± 1.8	.214

Values are mean ± SD, unless otherwise indicated.

CMR = cardiac magnetic resonance; EDV = end-diastolic volume; EDVi = end-diastolic volume indexed to body surface area; LVEDV = left ventricular end-diastolic volume; LVEDVi = left ventricular end-diastolic volume indexed to body surface area; LVEF = left ventricular ejection fraction; LVESV = left ventricular end-systolic volume; LVESVi = left ventricular end-systolic volume indexed to body surface area; NA = not applicable; RVEDV = right ventricular end-diastolic volume; RVEDVi = right ventricular end-diastolic volume indexed to body surface area; RVEF = right ventricular ejection fraction; RVESV = right ventricular end-systolic volume; RVESVi = right ventricular end-systolic volume indexed to body surface area; RVOT = right ventricular outflow tract.

**P*-value ≤ .05.

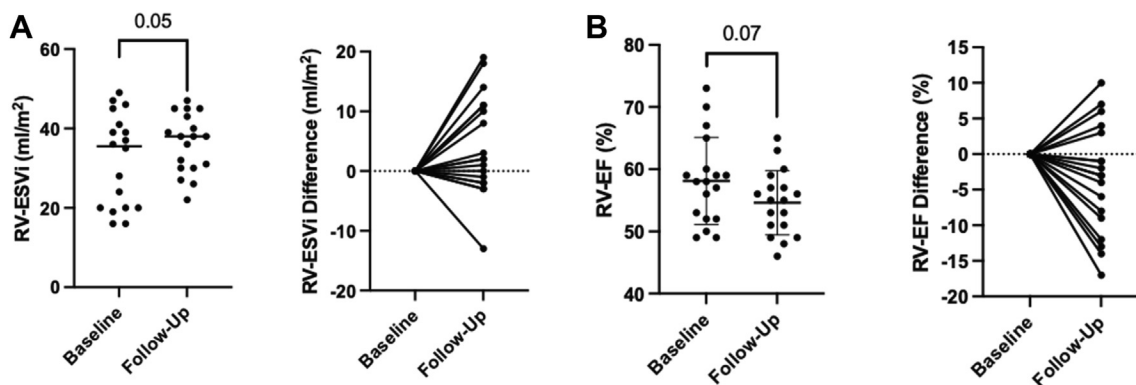


Figure 1 Volumetric changes in Brugada syndrome on longitudinal assessment. **A:** Increased right ventricular end-systolic volume indexed to body surface area (RVESVi) over the follow up period. **B:** A trend toward reduction in right ventricular ejection fraction (RVEF) on serial cardiac magnetic resonance.

(Figure 2). The LGE was localized to the septum in all cases, and specifically to the RV side of the basal septum in 3 patients. There was no evidence of diffuse fibrosis on follow-up scans with parametric mapping indices in the normal range (native T1 time 969.7 ± 36.7 ms and ECV $24.1 \pm 5.4\%$).

Patients exhibiting significant structural change during follow-up

The clinical and genetic features of patients with significant change in structural phenotype (ie, development of LGE and/or absolute reduction in RVEF of $\geq 10\%$) are described in Table 3. Among patients who developed LGE, 3 patients had a spontaneous type 1 pattern, and the average Shanghai score was 4.1, compared with 3.0 in the general cohort. Two of the 4 patients had a family history of BrS, but all were *SCN5A* negative. Among patients with a significant reduction in RVEF, 3 of 4 had an inducible type 1 BrS ECG (mean Shanghai score of 2.4). A disease-causing *SCN5A* variant

was present in patient TD3, part of a previously described family with a *SCN5A* translocation associated with pleiotropic manifestations including BrS, sudden cardiac death, sick sinus syndrome, and myocardial hypertrophy.²⁰ Otherwise, all patients who demonstrated significant structural changes during follow-up had no disease-causing variants identified on comprehensive cardiac genetic testing, analyzing genes associated with cardiomyopathy and inherited arrhythmia syndromes.

Discussion

Key findings

The key finding of this exploratory study is that structural abnormalities may evolve during follow-up of patients with BrS. We observed the development of focal replacement fibrosis evidenced by LGE in 22% of patients, as well as a reduction in RVESV and a trend toward reduction in RVEF over time. However, diffuse interstitial fibrosis was not detected on parametric mapping techniques. To our

Table 3 Characteristics of patients with significant progression of structural phenotype

Patient code	Structural abnormality	Age at follow-up scan (y)	Time between scans (y)	Ethnicity	Shanghai score	BrS ECG	FHx of BrS	Genetic testing	<i>SCN5A</i> Status
BPU1	LGE	50.5	4.6	Southern and Central Asian	6.5	Spontaneous	Yes	Genome	Negative
BPS1	LGE	46.6	5.4	North African and Middle Eastern	3.5	Spontaneous	Yes	Exome	Negative
ATT1	LGE	41.4	8.0	Northwest European	3.5	Spontaneous	No	Exome	Negative
BXI1	LGE	48.4	4.5	Northwest European	3	Fever induced	No	115-gene pan-cardiac panel	Negative
BTR1	RVEF reduction of 12%	52.2	3.9	Southeast Asian	2	Drug induced	No	100-gene pan-cardiac panel	Negative
TD3	RVEF reduction of 13%	40.8	4.5	Northwest European	2	Drug induced	No	Genome	Positive
CBX1	RVEF reduction of 14%	57.9	4.4	Northwest European	3.5	Spontaneous	No	Exome	Negative
CGL1	RVEF reduction of 17%	27.0	4.3	Northeast Asian	2	Drug induced	No	100-gene pan-cardiac panel	Negative

BrS = Brugada syndrome; ECG = electrocardiogram; FHx = family history; LGE = late gadolinium enhancement; RVEF = right ventricular ejection fraction.

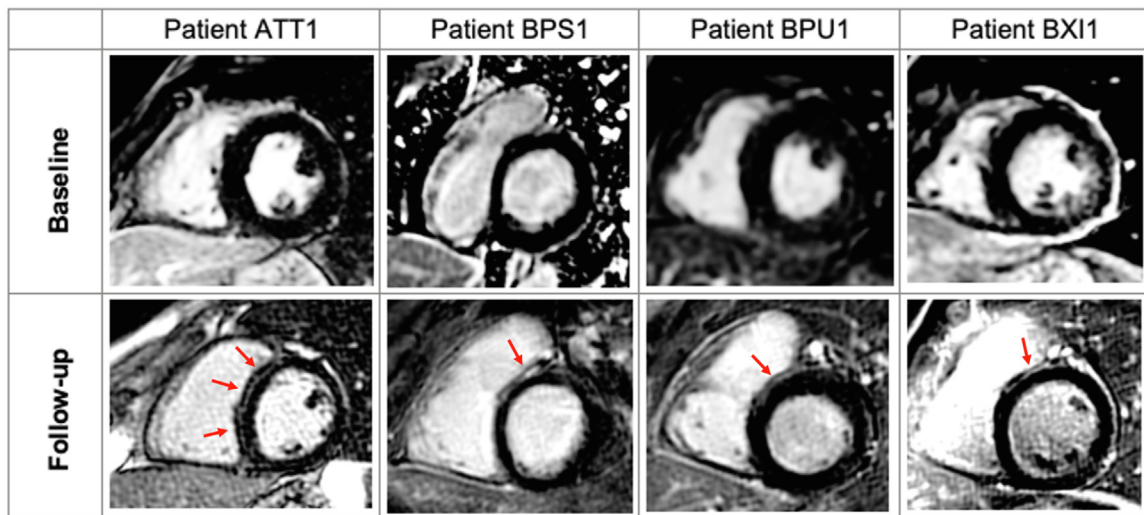


Figure 2 Late gadolinium enhancement (LGE) on cardiac magnetic resonance during follow-up in Brugada syndrome. Four patients developed LGE (indicated by red arrow) during the follow-up period, as demonstrated in these representative images (top row from baseline and bottom row from follow-up cardiac magnetic resonance). The most extensive LGE was seen in patient ATT1 with midwall enhancement in the septum. Patients BPS1, BPU1, and BXI1 developed LGE in similar distributions—on the right ventricular side of the basal septum.

knowledge, this is the first study to investigate whether the structural phenotype in BrS changes over time and also the first to report parametric mapping indices in a BrS cohort. Overall, these findings support the hypothesis that BrS has features of a cardiomyopathy with structural changes that may extend beyond the RVOT and, that these changes can progress over time, only becoming apparent with longitudinal assessment.

Histopathological substrate in BrS

Pathological studies of patients with BrS have reported a wide spectrum of abnormalities including interstitial fibrosis, inflammatory infiltrates, and fibrofatty replacement.^{4-6,21,22} Indeed, some findings have raised the possibility of overlap between the pathogenesis of BrS and other conditions such as arrhythmogenic cardiomyopathy and myocarditis.^{3,23} Epicardial and interstitial fibrosis and reduced gap junction expression have been shown to colocalize with the abnormal electrical substrate in the RVOT.^{4,5} However, myocardial changes are subtle and may be difficult to detect in with current noninvasive imaging technology.^{5,6,21} Indeed, Miles and colleagues²² identified increased collagen content throughout both the RV and LV (in the absence of overt histological abnormalities) on postmortem examination of 28 BrS decedents, confirming that even more subtle ultrastructural changes may be present on a global basis in BrS. These findings imply that BrS may actually be a generalized myocardial disease, with the intrinsic properties of the RVOT predisposing this region to more overt fibrosis and electrical abnormalities.⁵

Utility of CMR in BrS

As an extension of the pathological studies in BrS, CMR studies have also reported subtle changes in RV volumes

and contractile function compared with healthy control subjects as well as the presence of septal and LV LGE in some patients with BrS.^{9,10,14,24,25} The reported incidence of LGE is variable but is unequivocally lower than fibrosis in histological series, likely reflecting the lower sensitivity of CMR in detection of subtle fibrosis, as well as limitations of scar assessment in the thin-walled RV.

Development of structural changes during follow-up in BrS

The potential for progression in the structural phenotype of patients with BrS has not been systematically studied to date. Perhaps the most striking observation from the present study was the development of LGE in 4 of 18 patients that was not observed on their previous CMR imaging. The LGE was localized to the septum and confined to the midwall in all cases, thus not in a typically ischemic distribution. Midwall LGE is a typical finding in nonischemic dilated cardiomyopathy and has been associated with increased arrhythmic events.²⁶ Basal septal LGE has been reported in normal individuals, and while a physiological LGE pattern has been proposed, this pattern was not seen in the individuals who developed LGE in the present study.²⁷ The patients did not report any interval viral illness or chest pain syndrome to implicate myocarditis. Comprehensive cardiac genetic analysis excluded disease-causing genetic variants in cardiomyopathy (including desmosomal genes) or non-*SCN5A* channelopathy-associated genes in these patients.

We also observed an increase in RVESV and a trend toward reduced RVEF over time, suggesting that RV changes in BrS may also be a progressive process. This observation is in line with previous CMR studies that have demonstrated that RVESV is larger in patients with BrS compared with normal control subjects and associated with a reduction in

RVEF.^{9,14,24} However, we did not observe a significant change in RVOT volume in our small cohort. Perhaps provocative assessment of the RV following ajmaline infusion²⁵ or assessment of RV myocardial strain by CMR¹⁴ may further improve the sensitivity of detecting subclinical structural changes in the RV in BrS.

Potential mechanisms for structural progression in BrS

Mechanistic explanations for the observed development of abnormal tissue architecture in BrS may be speculated. First, we considered the interactions of age and *SCN5A* status. Patients with other inherited conditions such as HCM have been shown to have increased LGE with aging.¹³ In BrS, the cardiac sodium channel encoded by the *SCN5A* gene is known to interact with proteins in both the desmosome and gap junctions, and variants may cause a primary disturbance of myocardial structure.^{5,28,29} Moreover, *SCN5A* knockout mice have exhibited age-related development of fibrosis in ventricular myocardium and associated delay in epicardial activation.³⁰ While age is associated with increased ventricular fibrosis in these settings, it does not appear to be an adequate explanation in our cohort. The average age at the follow-up scan of those who developed fibrosis was 46.7 years compared with 47.6 years for those who did not. The age of those who developed LGE was also comparable to the mean age of patients without LGE in previous CMR studies of BrS (average mean age of 43.6 years, with a range of means from 38–48 years).^{9,10,14,24,25,31} *SCN5A* status did not appear to account for development of structural changes in our cohort, either. None of the 4 patients who developed LGE and only 1 of the 4 patients who developed significant reduction in RVEF had a pathogenic *SCN5A* variant.

Another potential explanation may be subclinical inflammation. Acute inflammation has been postulated as a potential mechanism for disease progression, and so-called hot phases in arrhythmogenic cardiomyopathy.^{32,33} In BrS, lymphocytic infiltration has been identified at sites with progression of electroanatomical substrate and in histological studies appears to associate with fibrosis.^{3,21,34} Elevated C-reactive protein and autoantibodies to cardiac proteins have been identified in BrS cohorts, and active myocardial inflammation detected by positron emission tomography scan was implicated in 2 patients with BrS with recurrent ventricular fibrillation, 1 of whom responded to immunosuppression, rather than antiarrhythmic medications and catheter ablation.^{35–37} Hence, myocardial inflammation may also have a role in pathogenesis, disease progression, and arrhythmogenesis in BrS.

Parametric mapping in BrS

Although LGE is validated as a correlate of replacement myocardial fibrosis, it has limitations for the detection of diffuse interstitial fibrosis. Newer parametric techniques such as T1 mapping and ECV assessment have been used to detect diffuse interstitial fibrosis in HCM, dilated

cardiomyopathy, and arrhythmogenic cardiomyopathy,^{38,39} but they have not been evaluated in patients with BrS to date.

Given the recent report of increased global collagen content in patients with BrS,²² we hypothesized that parametric mapping with CMR may allow in vivo detection of diffuse interstitial fibrosis in BrS. However, we did not detect any abnormal parametric mapping indices outside of the normal range. This may indicate that these techniques are insensitive to the detection of subtle increases in collagen deposition observed in histological evaluation of BrS. It is also possible that sampling the interventricular septum, one of the areas with relatively low distribution of collagen compared with the well-described fibrosis of the RVOT, reduces the sensitivity for detecting subtle interstitial fibrosis in BrS.²² Unfortunately, the thin wall of the RV, and particularly of the RVOT, renders advanced fibrosis assessment on these areas difficult with current noninvasive techniques.³⁹

Limitations

The findings from this study should be considered exploratory and hypothesis-generating because the study cohort was small. Replication of the results in a larger, multicenter cohort will be important to confirm these early findings. It is possible that an alternative diagnosis such as cardiomyopathy may explain the CMR changes; however, only patients with a spontaneous or drug-induced type 1 pattern were included (mean Shanghai score of 3), no patients had clinical symptoms suggestive of myocarditis, and there was no evidence of cardiomyopathy on the initial CMR scan or on comprehensive cardiac genetic testing. Baseline scans were performed at a number of sites with different protocols for image acquisition. Despite undertaking de novo analysis to standardize assessment, this real-world issue makes serial assessment more challenging. The time interval between CMR scans was not standardized, and a longer interval between scans may have the potential to reveal an even higher burden of progressive structural changes. Patients with an implantable cardioverter-defibrillator were excluded from this study, and it is possible that the degree of progressive structural change in BrS may be underestimated by our asymptomatic cohort.

Implications and future directions

BrS appears to be a progressive substrate in some patients, and changes may be detected on serial cardiac imaging. While Scheirlynck and colleagues²⁹ showed that patients with BrS and features of arrhythmogenic cardiomyopathy have worse arrhythmic outcomes, the clinical significance of progressive structural changes such as the development of focal fibrosis in BrS requires further evaluation. It will be useful for future studies to compare patients with and without progressive structural changes to understand demographic, genetic, and clinical differences and ultimately, outcomes. The mechanism for progressive changes should be explored, as this may have implications for therapy. In particular, serial evaluation of positron emission tomography–

computed tomography or inflammatory markers may shed light on the potential role of inflammation in disease progression. Although it remains to be seen whether disease progression is associated with poorer prognosis, it is plausible that it would have an impact on risk stratification, proposed therapies such as catheter ablation, and even immune modulation once the drivers of disease progression in these individuals are better understood.

Conclusion

Structural changes may emerge in a significant proportion of patients with BrS on longitudinal assessment. Subtle changes in RVESV and RVEF and the development of septal LGE over time suggest that there may be a degree of global myocardial dysfunction in BrS beyond the RVOT. The clinical significance of these progressive structural changes remains unclear, but if shown to be associated with adverse clinical outcomes in follow-up studies, they may dictate a change in the approach to risk stratification and clinical management of BrS.

Funding Sources: BG is the recipient of a National Health and Medical Research Council (NHMRC) Early Career Fellowship (#1122330). LY is the recipient of a co-funded National Heart Foundation of Australia and NHMRC PhD Scholarship (#102568 and #191351). CS is the recipient of an NHMRC Practitioner Fellowship (#1154992) and an NSW Health Cardiovascular Health Clinician Scientist Grant.

Disclosures: The authors have no conflicts to disclose.

Authorship: All authors attest they meet the current ICMJE criteria for authorship.

Patient Consent: Informed consent was obtained from all participants.

Ethics Statement: The study adhered to Helsinki Declaration guidelines and was approved by the local research ethics committee (X15-0061).

References

- Priori SG, Wilde AA, Horie M, et al. HRS/EHRA/APHS expert consensus statement on the diagnosis and management of patients with inherited primary arrhythmia syndromes. *Heart Rhythm* 2013;10:1932–1963.
- Krahn AD, Behr ER, Hamilton R, Probst V, Laksman Z, Han H-C. Brugada syndrome. *J Am Coll Cardiol EP* 2022;8:386–405.
- Frustaci A, Priori SG, Pieroni M, et al. Cardiac histological substrate in patients with clinical phenotype of Brugada syndrome. *Circulation* 2005;112:3680–3687.
- Ohkubo K, Watanabe I, Okumura Y, et al. right ventricular histological substrate and conduction delay in patients with Brugada syndrome. *Int Heart J* 2010;51:17–23.
- Nademanee K, Raju H, de Noronha SV, et al. Fibrosis, connexin-43, and conduction abnormalities in the Brugada syndrome. *J Am Coll Cardiol* 2015;66:1976–1986.
- Zumhagen S, Spieker T, Rolinck J, et al. Absence of pathognomonic or inflammatory patterns in cardiac biopsies from patients with Brugada syndrome. *Circ Arrhythm Electrophysiol* 2009;2:16–23.
- Catalano O, Antonaci S, Moro G, et al. Magnetic resonance investigations in Brugada syndrome reveal unexpectedly high rate of structural abnormalities. *Eur Heart J* 2009;30:2241–2248.
- Papavassiliu T, Veltmann C, Doesch C, et al. Spontaneous type 1 electrocardiographic pattern is associated with cardiovascular magnetic resonance imaging changes in Brugada syndrome. *Heart Rhythm* 2010;7:1790–1796.
- Bastiaenen R, Cox AT, Castelletti S, et al. Late gadolinium enhancement in Brugada syndrome: a marker for subtle underlying cardiomyopathy? *Heart Rhythm* 2017;14:583–589.
- Gray B, Gnanappa GK, Bagnall RD, et al. Relations between right ventricular morphology and clinical, electrical and genetic parameters in Brugada syndrome. *PLoS One* 2018;13:e0195594.
- Messroghli DR, Moon JC, Ferreira VM, et al. Clinical recommendations for cardiovascular magnetic resonance mapping of T1, T2, T2* and extracellular volume. *J Cardiovasc Magn Reson* 2017;19:75.
- Lorenzini M, Norrish G, Field E, et al. Penetrance of hypertrophic cardiomyopathy in sarcomere protein mutation carriers. *J Am Coll Cardiol* 2020;76:550–559.
- Habib M, Adler A, Fardini K, et al. Progression of myocardial fibrosis in hypertrophic cardiomyopathy: a cardiac magnetic resonance study. *J Am Coll Cardiol Img* 2021;14:947–958.
- Hohneck A, Overhoff D, Rutsch M, et al. Risk stratification of patients with Brugada syndrome: the impact of myocardial strain analysis using cardiac magnetic resonance feature tracking. *Hellenic J Cardiol* 2021;62:329–338.
- Riffel JH, Mayo R, Mueller-Hennessen M, Giannitsis E, Katus HA, Andre F. Age- and gender-related reference values of cardiac morphology and function in cardiovascular magnetic resonance. *Int J Cardiovasc Imaging* 2021;37:2011–2023.
- Petersen SE, Khanji MY, Plein S, Lancellotti P, Bucciarelli-Ducci C. European Association of Cardiovascular Imaging expert consensus paper: a comprehensive review of cardiovascular magnetic resonance normal values of cardiac chamber size and aortic root in adults and recommendations for grading severity. *Eur Heart J Cardiovasc Imaging* 2019;20:1321–1331.
- Zamorano JL, Lancellotti P, Rodriguez Munoz D, et al. 2016 ESC Position Paper on cancer treatments and cardiovascular toxicity developed under the auspices of the ESC Committee for Practice Guidelines. *Eur Heart J* 2016;37:2768–2801.
- Marwick TH. Ejection fraction pros and cons. *J Am Coll Cardiol* 2018;72:2360–2379.
- Richards S, Aziz N, Bale S, et al. Standards and guidelines for the interpretation of sequence variants. *Genet Med* 2015;17:405–424.
- Yeates L, Ingles J, Gray B, et al. A balanced translocation disrupting SCN5A in a family with Brugada syndrome and sudden cardiac death. *Heart Rhythm* 2019;16:231–238.
- Pieroni M, Notarstefano P, Oliva A, et al. Electroanatomic and pathologic right ventricular outflow tract abnormalities in patients with Brugada syndrome. *J Am Coll Cardiol* 2018;72:2747–2757.
- Miles C, Asimaki A, Ster IC, et al. Biventricular myocardial fibrosis and sudden death in patients with Brugada syndrome. *J Am Coll Cardiol* 2021;78:1511–1521.
- Corrado D, Nava A, Bujá G, et al. Familial cardiomyopathy underlies syndrome of right bundle branch block, ST segment elevation and sudden death. *J Am Coll Cardiol* 1996;27:443–448.
- Rudic B, Schimpf R, Veltmann C, et al. Brugada syndrome: clinical presentation and genotype-correlation with magnetic resonance imaging parameters. *Europace* 2016;18:1411–1419.
- Pappone C, Santinelli V, Mecarocci V, et al. Brugada syndrome: new insights from cardiac magnetic resonance and electroanatomical imaging. *Circ Arrhythm Electrophysiol* 2021;14:e010004.
- Halliday BP, Gulati A, Ali A, et al. Association between midwall late gadolinium enhancement and sudden cardiac death in patients with dilated cardiomyopathy and mild and moderate left ventricular systolic dysfunction. *Circulation* 2017;135:2106–2115.
- Joncas SX, Kolman L, Lydell C, et al. Differentiation of physiologic versus pathologic basal septal fibrosis. *J Cardiovasc Magn Reson* 2014;16:P104.
- Sato PY, Coombs W, Lin X, et al. Interactions between ankyrin-G, Plakophilin-2, and connexin43 at the cardiac intercalated disc. *Circ Res* 2011;109:193–201.
- Scheirlynck E, Chivulescu M, Lie OH, et al. Worse prognosis in Brugada syndrome patients with arrhythmogenic cardiomyopathy features. *J Am Coll Cardiol EP* 2020;6:1353–1363.
- Jeevaratnam K, Poh Tee S, Zhang Y, et al. Delayed conduction and its implications in murine Scn5a(+/-) hearts: independent and interacting effects of genotype, age, and sex. *Pflugers Arch* 2011;461:29–44.
- Tessa C, Del Meglio J, Ghidini Ottonelli A, et al. Evaluation of Brugada syndrome by cardiac magnetic resonance. *Int J Cardiovasc Imaging* 2012;28:1961–1970.
- Smith ED, Lakdawala NK, Papoutsidakis N, et al. Desmoplakin cardiomyopathy, a fibrotic and inflammatory form of cardiomyopathy distinct from typical dilated or arrhythmogenic right ventricular cardiomyopathy. *Circulation* 2020;141:1872–1884.
- Tung R, Bauer B, Schelbert H, et al. Incidence of abnormal positron emission tomography in patients with unexplained cardiomyopathy and ventricular

- arrhythmias: the potential role of occult inflammation in arrhythmogenesis. *Heart Rhythm* 2015;12:2488–2498.
34. Notarstefano P, Pieroni M, Guida R, et al. Progression of electroanatomic substrate and electric storm recurrence in a patient with Brugada syndrome. *Circulation* 2015;131:838–841.
 35. Li A, Tung R, Shivkumar K, Bradfield JS. Brugada syndrome-Malignant phenotype associated with acute cardiac inflammation? *HeartRhythm Case Rep* 2017;3:384–388.
 36. Bonny A, Tonet J, Marquez MF, et al. C-reactive protein levels in the Brugada syndrome. *Cardiol Res Pract* 2011;2011:341521.
 37. Chatterjee D, Pieroni M, Fatah M, et al. An autoantibody profile detects Brugada syndrome and identifies abnormally expressed myocardial proteins. *Eur Heart J* 2020;41:2878–2890.
 38. Dass S, Suttie JJ, Piechnik SK, et al. Myocardial tissue characterization using magnetic resonance noncontrast t1 mapping in hypertrophic and dilated cardiomyopathy. *Circ Cardiovasc Imaging* 2012;5:726–733.
 39. Georgiopoulos G, Zampieri M, Molaro S, et al. Cardiac magnetic resonance in patients with ARVC and family members: the potential role of native T1 mapping. *Int J Cardiovasc Imaging* 2021;37:2037–2047.